Climatology and Change of Extreme Precipitation Events in Taiwan Based on Weather Types

Yi-chao Wu[a,*], S.-Y. Simon Wang[b,c], Yi-Chiang Yu[a], Chu-Ying Kung[a], An-Hsiang Wang[a], Sebastian A. Los[c], Wan-Ru Huang[d]

[a]*Meteorology Division, National Science and Technology Center for Disaster Reduction, New Taipei, Taiwan*

[b]*Utah Climate Center, Utah State University, Logan, UT, USA*

[c]*Department of Plants, Soils, and Climate, Utah State University, Logan, UT, USA*

[d]*Department of Earth Sciences, National Taiwan Normal University, Taipei, Taiwan*

***Corresponding Author:** Yi-chao Wu

Meteorology Division, National Science and Technology Center for Disaster Reduction, 9F., No.200, Sec. 3, Beisin Rd., Xindian District, New Taipei City, 23143, Taiwan

Telephone: +886-2-8195-8633 E-mail: yichaowu@ncdr.nat.gov.tw

Keywords:

Climatology; Extreme Precipitation; Taiwan; Weather Type

Abstract

Taiwan's most significant natural hazards are caused by hydrological extremes resulting from excessive precipitation. The threat of extreme precipitation is posed by several different types of weather patterns that affect Taiwan. This study examined the bi-decadal changes in rainfall by defining an extreme precipitation occurrence (EPO) for a range of event durations from 1 to 24 hours. Three major weather types affecting EPO in Taiwan were identified from 1993 to 2015: the front-type consisting of either a frontal zone or convective systems developing with an apparent Meiyu cloudband, diurnal rainfall events when no apparent synoptic features are present, and a tropical cyclone (TC) type according to the maximum sustained wind radius of a TC. Results show that TC-type events have the greatest overall contribution to EPO at longer (>6h) durations. Diurnal/afternoon convection events contribute most to the shorter (< 3h) duration EPO, while frontal/Meiyu systems prevail in the medium (3-6h) duration. EPO of almost all durations have experienced an increasing trend, with the 3h and 12h EPO having increased by 4.6 days each over the 23 years. The distinction between EPO trends for the entire island of Taiwan and for the Taipei metropolitan area alone (northern Taiwan, population of 7 million) were compared, and an intriguing interannual variation is reported in the TC-type EPO associated with the TC season one year to a year and half just before an ENSO event. The analysis here provides refined statistical distributions of extreme rainfall and these can contribute to the revision of governmental definitions for weather disasters that are used in mitigation and response strategies.

1. Introduction

In terms of natural disasters, the World Bank ranks Taiwan as having the highest mortality risk, highest economic risk, and as being most exposed to "multiple hazards" than any other country (Dilley et al. 2005). Taiwan's most significant natural hazards are caused by hydrological extremes resulting from excessive precipitation. Located within both the summer and winter monsoons of East Asia, Taiwan faces an extreme precipitation threat year-round and has experienced an increasing trend in heavy rains (Tu and Chou 2013). Since tropical cyclones (TCs) contribute significantly to Taiwan's annual rainfall (Chen et al. 2010; Wang and Chen 2008), many studies have focused on TC-induced precipitation extremes (Chen et al. 2013) and their long-term change (Chang et al. 2013; Chu et al. 2014; Liang et al. 2017; Ren et al. 2006; Wu et al. 2016). The most robust increases in TC rainfall have been found on mountainous terrain due to the tendency for slower-moving TCs to interact with the high mountains (Tu and Chou 2013). Though some recent studies have explored changes in Taiwan's extreme precipitation characteristics (Hsu and Chen 2002; Yeh and Chen 1998), one factor that has been overlooked is how the diversity of weather types affecting Taiwan are each impacting changes in extreme precipitation.

Several different types of weather phenomena can pose an extreme precipitation threat in Taiwan. The East Asian summer monsoon (EASM) creates a distinct onset-break-revival-withdrawal lifecycle in Taiwan's summer rainfall (Chen et al. 2004) and each phase of this cycle features 1-2 dominant types of weather system (Chen and Chen 2003; Wang and Chen 2008). In the monsoon onset/active phase, frontal systems produce mesoscale convective systems while enhancing thermally-induced local convection (Huang and Chen 2015; Wang et al. 2004), the combination of which increases the odds of extreme rainfall during this Meiyu season (Xu et al. 2009). The monsoon break following the Meiyu season is characterized by active afternoon thunderstorms that develop along Taiwan's western mountain slopes. These diurnal thunderstorms can cause flash flooding and account for up to 60% of break-phase rainfall (Wang and Chen 2008). In light of these overall patterns in extreme precipitation, the extent to which each weather type and its associated extreme precipitation has changed in time has not been well documented.

In this paper, we analyzed Taiwan's extreme precipitation by categorizing station rainfall observations by various event durations and weather types. The goal of this study is to provide refined climatological distributions of extreme rainfall that support the government's efforts in redefining its criteria for weather related disasters in order to address the growing need for improved disaster prevention and adaptation strategies. Based on previous methods of classifying Taiwan's rainfall climatology with respect to different weather systems (Chen and Chen 2003; Wang and Chen 2008), here we examined the variability and change in extreme precipitation associated with the major weather types.

2. Data and Methodology

a. Data and quality control

Most previous studies examining rainfall trends in Taiwan have utilized its high density network of precipitation monitoring stations that was established on the island in the early 1990s (Kuo et al. 2016; Wu et al. 2016) comprised of nearly 600 automated rain gauges to date (Fig. 1a). When seeking to detect change in precipitation over time, data quality becomes crucial. Because many stations are located in remote mountains and valleys and therefore relay observations through radio waves, it is not uncommon for the signal of certain stations to become attenuated during heavy-rain events (when the transmission is most crucial). When signal is lost, a code appears in the raw data indicating a missing value; but when the signal resumes, the station transmits the rainfall amount accumulated over those missing hours (instead of the rainfall for the hour of resumed communication alone). This creates false short-duration heavy rainfall that can skew the distribution of precipitation extremes.

Here, precipitation record errors due to these radio telemetry issues in Taiwan's automated rain gauge network were identified and removed. For example, an erroneous record of extreme precipitation is displayed in Figure 2b, which shows a large precipitation reading on 13 October 1999 from station C0T960 in eastern Taiwan. Two signs indicate error in this reading: 1) no systematic pattern is apparent in the rainfall map (Figure 2a) and 2) a period of continuous missing communication (coded -9996) is noted in the station's record leading up to the large rainfall amount (Figure 2c). To detect this type of recording error, an algorithm-based method using similar criteria was used to review the hourly precipitation data for each of the 592 stations over the 23-year period of 1993-2015, amounting to 5 million data points being examined. Subsequently, about 230,000 data points were "flagged" and removed. These errors account for only 0.18% of the entire data set. However, when considering the identification of far-tail extremes in precipitation, this number could become significant.

An additional issue arises regarding the application of trend analysis when individual stations have variable periods of record (Wu et al. 2016). The number of automated rain gauges in Taiwan has grown from about 200 to over 550 in the period from 1993 to 2015 (Fig. 1b). Additionally, some stations were only temporarily established (for a special period of interest), while some failed or were discontinued over the course of the 23 years. Of the 592 stations, only 135 provide continuous observations, with at least 97.5% of data coverage, since 1993 and these stations are indicated in Fig. 1a. Therefore in the following analyses, all 592 stations were used for the climatological examination of precipitation extremes, but only the 135 consistent stations were used for detecting changes over time in order to maintain the rigor of the trend analysis.

b. Extreme precipitation threshold

Extreme precipitation was defined for six durations of 1, 2, 3, 6, 12, and 24 hours (h). For 1h precipitation, we selected *only one* maximum hourly precipitation from all available stations during each day. These 1h precipitation values formed a gamma distribution of 8,109 rainy days over the 23 years, defined as at least one station with daily rainfall exceeding 1mm. An extreme precipitation threshold was then given as two standard deviations (in mm) above the mean of the maximum 1h values, equivalent to events that rank as the top 3.9% among all records, or the 95th percentile. Any day that was marked by this 1h extreme precipitation occurrence in at least one station was denoted as 1h EPO hereafter. Hence, the EPO value for a day is either *one* or *zero*. The same approach was applied for the 2h, 3h, 6h, 12h, and 24h durations to include extreme events that occurred in less than 5% of the total rainy days. By this definition, a day defined as the 1h EPO may or may not be included in the 24h EPO, and vice versa. On the other hand, longer-duration EPO could include hours also of shorter-duration EPO.

Different types of natural disaster are associated with differing durations of extreme precipitation. For example, Caine (1980) has shown that shallow landslides are often linked to rainfall accumulated over an extended period of time and that 60% of debris flow cases are caused by heavy rainfall accumulated over 6 hours or longer. Examples of this association have been noted in Taiwan, such as the debris flows and landslides caused by Typhoon Morakot (2009) (Jan et al. 2011). On the other hand, flash floods, characterized by their rapid development, are often linked to short (<6h) duration extreme precipitation (Hapuarachchi et al. 2011). Therefore, key to providing disaster early warnings is accurate climatological information concerning extreme precipitation of various durations. The aforementioned corrections to data biases in precipitation observations hence become crucial, particularly for short-duration precipitation.

c. Categorization of weather types

It is well documented that a range of different weather event types can affect Taiwan. The majority of active weather in Taiwan consists of synoptic frontal patterns, tropical cyclones, and, when no apparent large-scale weather systems are present, diurnal/afternoon thunderstorms (Huang and Chen 2015; Kuo et al. 2016; Wang and Chen 2008). Based on the synoptic depiction of common weather types by the National Science and Technology Center for Disaster Reduction (NCDR)[1] and using weather maps produced by Taiwan's Central Weather Bureau (CWB), we determine the major type of weather that contributed to daily rainfall events from 1993 to 2015. As with previous studies that have categorized different types of weather in Taiwan (Huang and Chen 2015; Kuo et al. 2016; Wang and Chen 2008), we focused on three main types: (i) the front-type consisting of either a frontal zone within the domain of 119º-122ºE, 21º-26ºN encompassing Taiwan, as depicted on the CWB's synoptic charts, or convective systems developing within an apparent Meiyu cloudband as noted on CWB's infrared satellite and radar imagery, (ii) diurnal rainfall events when no apparent synoptic systems were present in the vicinity of Taiwan, i.e. within the domain of 119º-122ºE, 21º-26ºN; (iii) a tropical cyclone type when some or all of Taiwan fell within the maximum sustained wind radius of one or more TCs (including tropical depressions), based upon CWB's infrared imagery and TC track record. The diurnal type of rainfall events is identified as when i) the major rainfall peak was detected in an afternoon/evening (1200–2100 LST), ii) no rainfall was detected in the morning (0600–1100 LST) of that day, and iii) synoptically inactive conditions were present around Taiwan (21-26°N, 119-122°E). Here, synoptic inactivity means a lack of convective clouds or frontal bands over the island before the afternoon/evening convection occurs, thereby excluding potential effects from any synoptic weather systems (fronts, tropical disturbances, etc.). This procedure follows the "diurnal category" definition in Wang and Chen (2008). Examples of these three main weather types are shown in Supplemental Figure S1 along with a 24h precipitation map with a further description. We note that while Wang and Chen (2008) divided the Meiyu-type

[1] http://www.ncdr.nat.gov.tw/Files/image/20150720174726115/files/120.pdf (in Chinese)

weather into fronts and Meiyu rainstorms, these two weather systems are combined in the present analysis.

A fourth type, namely *other* weather system(s), categorizes the days that do not belong to any of these three main types of weather. These other-type weather systems include complicated terrain-flow interactions, weak tropical disturbances, and winter monsoon affecting Taiwan, according to Wang and Chen (2008) and a NCDR report[1]. However, each of these weather-type categories has a small sample size that prohibited meaningful trend analysis. Thus, the extreme precipitation thresholds defined in Section 2b were applied to these four weather types when analyzing trends.

3. Results

a. Seasonal distribution

The 23-year accumulated EPO frequency (in days) and the accumulated maximum precipitation for each duration are shown in Figures 3a and 3b respectively, with colors denoting the four weather types. With increasing duration length, a decreased total number of EPO events is apparent for the diurnal-type EPOs versus an increased total number of EPO events of the TC-type. This result is expected because synoptically driven events like TCs produce longer and subsequently more accumulated rainfall, while the afternoon thunderstorms typically develop and dissipate within a few hours leading to short-duration rainfall (Kishtawal and Krishnamurti 2001; Lin et al. 2011). The front-type's extreme precipitation frequency appears in between the diurnal and TC types, having the highest frequency at 3h and 6h. The "other" weather types rank second in the contribution to Taiwan's annual extreme rainfall days. In terms of contribution to the accumulated maximum precipitation of these extreme events, TC-type EPOs rank first and the "other" type second. The proportions of TC-type EPO contribution rise with increasing duration length.

Based on the 1993-2015 climatology, an average of 16.8 days of extreme precipitation from any duration category occur during a given year. The annual distribution of EPO is shown in Figs. 4a and 4b for 15-day intervals, where colors represent different durations. For a better illustration, the 6 durations are separately shown in two panels: 1h, 2h, and 3h EPO in Fig. 4a and 6h, 12h, and 24h EPO in Fig. 4b. The same is done for subsequent figures Fig. 5 – Fig. 9. Highest EPO values are found across the warm season as expected. May-June is marked by a sharp increase in EPO followed by short period of reduced EPO in late June (Fig. 4a, b). This evolution of EPO presents an interesting subseasonal feature that apparently follows the subseasonal progression of the East Asian summer monsoon (Chen et al. 2004). The May-June increase of the 3h EPO is distinctly larger than those for the other EPOs, supporting the dominance of front-type weather given its 3h peak as shown in Fig. 3a. A second subseasonal peak in EPO, the annual maximum for all durations, occurs during the first half of August (Fig. 4a, b). While this appears as a sharp peak for almost all durations, the 1h EPO delineates a more spread distribution during the typhoon season (July-September) than other categories (Fig. 4a). The 6h, 12h, and 24h EPOs then show additional peaks during the early October period (Fig. 4b).

For comparison we show in Fig. 4c long-term pentad (5-day) precipitation of global satellite/gauge composite precipitation data (GPCP; Adler et al. 2003) averaged from the four grids covering the Taiwan domain. This pentad mean precipitation time series shows the distinct EASM lifecycle experienced by Taiwan, comprised of the active, break, revival and retreat phases of the subseasonal evolution (Chen et al. 2004). The monsoon revival phase coincides with the largest frequency of TCs (Fig. 4d), especially those below Category 4 on the Saffir-Simpson wind scale. Visual inspection of Figs. 4a/b and 4c finds high coherency between the two, indicating that the subseasonal evolution of EPO in Taiwan closely follows that of the EASM lifecycle. This result has implications for understanding the weather types and seasonal properties of EPO as discussed next.

b. Bi-decadal changes

Figure 5 shows the temporal distribution and linear trend across Taiwan of the (a) annual accumulated EPO, (b) pre-monsoon season EPO for May and June, (c) summer season EPO for July-September, and (d) autumn season EPO for October through November. The three seasons were classified based upon the patterns in Taiwan's subseasonal rainfall distribution in Fig. 4c. Marked interannual variability appears in EPO during all seasons, while overall increasing trends are observed for the pre-monsoon and summer season EPO values. The apparent decadal-scale variability in the summer EPO is noteworthy, delineated by less extreme precipitation events during 1993-2002, more events in 2003-2009, and less again after 2010. Different durations exhibit slightly different, yet overall coherent year-to-year variations with similar trends. Table 1 summarizes the slopes of the trend analysis of each EPO duration, with the various significance levels indicated (per Student's *t*-test). In summer and autumn, significant trends ($p<0.1$) are observed in the EPO for the 2-12h durations. In the pre-monsoon season, only the 12h duration shows a significant increase ($p<0.1$), albeit with a weaker increasing trend. In autumn, shorter durations exhibit more significant decreasing trends. Throughout the year, marginally significant upward trends are only seen in 3h and 12h.

Following the analyses outlined in Section 2c, we next categorized the EPO trends into the four described weather types. As shown in Table 1, the TC-type extreme precipitation shows a universal significant increase in all durations during summer, except 1h. This finding is in good agreement with the previous studies that have found general increases in TC-related rainfall over Taiwan (Chang et al. 2013; Chu et al. 2014; Liang et al. 2017; Tu and Chou 2013). By contrast, the autumn TC-type EPO reveals an overall decreasing trend among all durations, though not significant. A separate examination of the other types of weather (not shown) in autumn indicates consistent but insignificant downward trends, aiding the more significant downward trends found in all the weather types.

In terms of the annual variation in EPO, the front and diurnal types of weather do not reveal any significant trends, except for a slight increase in the 1h diurnal type (Table 1). Figure 6 shows the EPO time series of the different weather types for their most active season. Though not shown here, the spatial distribution of EPO changes of different rain gauge stations (computed in terms of regression slopes) agrees with previous studies such as the observation by Tu and Chou (2013) and Wu et al. (2016) that the majority of extreme precipitation and associated increases occur over the western and southwestern slopes of the Central Mountain Range in Taiwan, due to terrain enhancement of synoptic flows.

c. Difference between Taipei and the rest of Taiwan

During the pre-monsoon season, it is not uncommon for Taiwan to experience a contrast in weather systems between northern and southern Taiwan, due to the narrow meridional thermal gradient associated with zonally oriented frontal zones across the island (Huang and Chen 2015). The metropolitan area of Taipei consists of Taipei City, capital of Taiwan, and the surrounding cities that together form what is known as "New Taipei" (Fig. 1a). The basin that encompasses Taipei City and New Taipei is inhabited by around 7 million people, accounting for 34% of Taiwan's total population. Given its relative importance in population, economy, as well as climatological differences from the rest of Taiwan such as a strong heat-island effect (Chen et al. 2007), we decided to conduct a separate EPO trend analysis for Taipei.

By using the rain gauges within the boundary of New Taipei (Fig. 1a inset) and following the procedure in Section 2a, we derived a different set of EPO that is referred simply as Taipei hereafter. As shown in Fig. 7 and Table 2, the pre-monsoon season has shown an increase in EPO and this increase is more pronounced at longer durations, a feature not reflected in the rest of Taiwan (Fig. 5). The 24h EPO has increased with the highest significance ($p<0.01$). As shown in Table 2 and Figure 8, the front-type extreme precipitation has increased in Taipei at most durations.

Summertime EPO for Taipei also shows a moderate increase, with the largest contribution to this increase coming from the diurnal and TC- types (Table 2). The increasing trend in diurnal-type EPO is arguably linked to the documented increases in the afternoon thunderstorm frequency and intensity over Taipei that is likely associated with the urban heat island effect (Chen et al. 2007; Kataoka et al. 2009). Moreover, increased nighttime temperatures associated with urban heat island can help to destabilize the lower troposphere (Shiu et al. 2009), which could be conducive for thermally driven convection. The autumn EPO for Taipei shows a uniform and moderate decrease across all durations with a significant reduction at 3h, and these downward trends are consistent with those associated with TCs (Table 2). The trends in other types of EPO are minor and insignificant. These results highlight the consistent trends in extreme precipitation with respect to the dominant weather type(s), time of year, and region.

d. Interannual variation

Even though the increasing trends in TC-type EPO are consistent with previous studies of TC rainfall, here we report a previously undocumented feature in the interannual variation of extreme precipitation related to TCs. In the western North Pacific, TC frequency fluctuates considerably at the interannual timescale and this is largely driven by the El Niño–Southern Oscillation (ENSO) (Chen et al. 2006; Du et al. 2011; Jiang and Zipser 2010). However, we found that the precursor years of ENSO (i.e. about 1-1.5 year before the mature phase of an ENSO event) appear to affect the TC-type EPO in Taiwan, as well. We designated ENSO years by following the NOAA Climate Prediction Center definitions of an El Niño or a La Niña event based on a threshold of +/- 0.5^{o}C for the winter Oceanic Niño Index (ONI). For example, 1997 is defined as the El Niño year for the 1997-98 El Niño, 1988 for the 1988-89 La Niña, and so forth. Using this definition, the TC season of an El Niño "precursor year" corresponds to 15-18 months preceding the El Niño winter, denoted as El Niño-1 (and likewise for La Niña-1).

Figure 9a and Fig. 9b show the annual TC-type EPO of 6 durations marked with ENSO years by colored bars, where orange bars correspond to El Niño periods and blue bars for La Niña. The highest values for TC-type EPO at 12h and 24h durations do not correlate with El Niño; instead we noticed a robust tendency for increased TC-type EPO in the years *before* El Niño, with the exception of 1993, 2003, and 2014. However, one-half of the lowest EPO years did occur during La Niña years. In Fig. 9c and Fig. 9d, we plotted the TC-type EPO for all years, El Niño/La Niña years, and their precursor years (El Niño-1/La Niña-1) for the 12h and 24h durations. Interestingly, the difference between El Niño-1 and all years is significant ($p<0.05$ via a non-parametric test), and those between La Niña-1 and all years and between La Niña and all years are even more significant ($p<0.01$). This is the case for both 12h and 24h durations. By comparison, there is not a significant difference between El Niño and all years.

The causes for this contrast in the TC-type EPO between El Niño-1 and La Niña-1 years are likely manifold and requires further research. ENSO events are typically preceded by favorable wind forcing and sea surface temperature anomalies (SSTA) that form up to one year before the triggering of the event (Capotondi and Sardeshmukh 2015). It is possible that the linkage reported here between ENSO precursor years and TC occurrences near Taiwan is related to the systematic patterns in SST and low-level circulation anomalies associated with an ENSO precursor. One prominent ENSO precursor relevant to Taiwan is the so-called western North Pacific (WNP) pattern, which is defined by a dipole of SSTA and wind patterns between the areas to the east of Taiwan and areas to the northeast of Papua New Guinea (Pegion and Selman 2017; Wang et al. 2012, 2013). However, the connection between ENSO precursors and increased TC-type EPO remains speculative because, after plotting composite SSTA and wind differences between El Niño-1 and La Niña-1 (Fig. S2), the results did not reveal any consistent or robust patterns in the WNP during the TC season. This lack of direct association may be due to the fact that the WNP pattern is mainly a winter phenomenon while TCs primarily occur in warm season. Currently, we do not have any explanation as to what causes the significant contrast in the TC-type EPO between El Niño-1 and La Niña-1 years. Exploring the physical cause of this phenomenon deserves further attention but is beyond the scope of this study.

4. Concluding Remarks

Based on 135 rainfall stations in Taiwan that have provided consistent observations since 1993 (with at least 97.5% of data coverage), the change in extreme precipitation occurrence (EPO) was analyzed. The analysis of EPO was further categorized by six durations (1, 2, 3, 6, 12, and 24 hours) and sorted by four major weather types. There are on average 16.8 EPO days for all of Taiwan per year. Of these 16.8 days, TCs show the greatest overall contribution to EPO through the year, particularly at longer (>6h) durations. Diurnal/afternoon convection events contribute more to the shorter (< 3h) duration EPO, while frontal/Meiyu systems do so in the medium (3-6h) duration of EPO. Regarding bi-decadal changes, almost all durations of EPO have experienced an increasing trend (except for 1h), with the 3h and 12h trends being the most significant, having increased by 4.6 days over the last 23 years. We note that short (<6h) duration extreme precipitation events are often linked to flash flooding, while long (>12h) duration ones frequently can trigger landslides and debris flows on Taiwan's sloping terrain. Therefore, the trend analysis presented here has important implications for the future occurrence of extreme precipitation-related disasters. The increases in diurnal-type and front-type EPO are greater in the Taipei metropolitan area than the whole island, signaling an increasing risk of extreme precipitation on life and property in a large, densely-populated urban area.

Improving the predictability of extreme precipitation threat has been called for by the IPCC report *Managing the Risks of Extreme Events and Disasters to Advance Climate Change Adaptation* (Field 2012) and also subsequent extreme event studies as reviewed by the U.S. National Academies of Sciences and Medicine (2016). The NCDR of Taiwan monitors and reviews the extreme precipitation threat in order to establish consistent, physically sound thresholds that can be used collectively by the hydrology, construction, environmental protection, and disaster prevention sections of the government. Thus, the results of this study are potentially useful for the greater societal goal of disaster prevention by informing those responsible for implementing timely and necessary mitigation actions of the changing characteristics of extreme precipitation.

Acknowledgements:

SYW was supported by DOE grant DESC0016605.

References

Adler, R. F., and Coauthors, 2003: The Version-2 Global Precipitation Climatology Project (GPCP) Monthly Precipitation Analysis (1979,ÄìPresent). *Journal of Hydrometeorology*, **4,** 1147-1167.

Caine, N., 1980: The rainfall intensity-duration control of shallow landslides and debris flows. *Geografiska Annaler. Series A, Physical Geography*, **62, No. 1/2**, pp. 23-27.

Capotondi, A., and P. D. Sardeshmukh, 2015: Optimal precursors of different types of ENSO events. *Geophysical Research Letters*, **42,** 9952-9960.

Chang, C.-P., Y.-T. Yang, and H.-C. Kuo, 2013: Large increasing trend of tropical cyclone rainfall in Taiwan and the roles of terrain. *Journal of Climate*, **26,** 4138-4147.

Chen, C.-S., and Y.-L. Chen, 2003: The rainfall characteristics of Taiwan. *Monthly Weather Review*, **131,** 1323-1341.

Chen, J.-M., T. Li, and C.-F. Shih, 2010: Tropical cyclone–and monsoon-induced rainfall variability in Taiwan. *Journal of Climate*, **23,** 4107-4120.

Chen, J.-M., P.-H. Tan, and C.-F. Shih, 2013: Heavy rainfall induced by tropical cyclones across northern Taiwan and associated intraseasonal oscillation modulation. *Journal of Climate*, **26,** 7992-8007.

Chen, T.-C., S.-Y. Wang, and M.-C. Yen, 2006: Interannual Variation of the Tropical Cyclone Activity over the Western North Pacific. *Journal of Climate*, **19,** 5709-5720.

——, 2007: Enhancement of Afternoon Thunderstorm Activity by Urbanization in a Valley: Taipei. *Journal of Applied Meteorology and Climatology*, **46,** 1324-1340.

Chen, T.-C., S.-Y. Wang, W.-R. Huang, and M.-C. Yen, 2004: Variation of the East Asian Summer Monsoon Rainfall*. *Journal of Climate*, **17,** 744-762.

Chu, P. S., D. J. Chen, and P. L. Lin, 2014: Trends in precipitation extremes during the typhoon season in Taiwan over the last 60 years. *Atmospheric Science Letters*, **15,** 37-43.

Dilley, M., and Coauthors, 2005: Natural Disaster Hotspots: A Global Risk Analysis, 148 pp.

Du, Y., L. Yang, and S.-P. Xie, 2011: Tropical Indian Ocean influence on Northwest Pacific tropical cyclones in summer following strong El Niño. *Journal of Climate*, **24,** 315-322.

Field, C. B., 2012: *Managing the risks of extreme events and disasters to advance climate change adaptation: special report of the intergovernmental panel on climate change.* Cambridge University Press.

Hapuarachchi, H. A. P., Q. J. Wang, and T. C. Pagano, 2011: A review of advances in flash flood forecasting. *Hydrol. Process.*, **25**, 2771–2784. doi: 10.1002/hyp.8040

Hsu, H.-H., and C.-T. Chen, 2002: Observed and projected climate change in Taiwan. *Meteorology and Atmospheric Physics*, **79,** 87-104.

Huang, W.-R., and K.-C. Chen, 2015: Trends in pre-summer frontal and diurnal rainfall activities during 1982–2012 over Taiwan and Southeast China: characteristics and possible causes. *International Journal of Climatology*, **35,** 2608-2619.

Jan, C. D., Y. C. Hsu, J. S. Wang, and W. S. Huang, 2011: Debris flows and landslides caused by typhoon Morakot in Taiwan. *5th International Conference on Debris-Flow Hazards Mitigation: Mechanics, Prediction and Assessment, Padua, Italy*, pp. 675-683.

Jiang, H., and E. J. Zipser, 2010: Contribution of tropical cyclones to the global precipitation from eight seasons of TRMM data: Regional, seasonal, and interannual variations. *Journal of climate*, **23,** 1526-1543.

Kataoka, K., F. Matsumoto, T. Ichinose, and M. Taniguchi, 2009: Urban warming trends in several large Asian cities over the last 100 years. *Science of The Total Environment*, **407,** 3112-3119.

Kishtawal, C., and T. Krishnamurti, 2001: Diurnal variation of summer rainfall over Taiwan and its detection using TRMM observations. *Journal of Applied Meteorology*, **40,** 331-344.

Kuo, Y.-C., M.-A. Lee, and M.-M. Lu, 2016: Association of Taiwan's rainfall patterns with large-scale oceanic and atmospheric phenomena. *Advances in Meteorology*, **2016**.

Liang, A., L. Oey, S. Huang, and S. Chou, 2017: Long-term trends of typhoon-induced rainfall over Taiwan: In situ evidence of poleward shift of typhoons in western North Pacific in recent decades. *Journal of Geophysical Research: Atmospheres*, **122,** 2750-2765.

Lin, P.-F., P.-L. Chang, B. J.-D. Jou, J. W. Wilson, and R. D. Roberts, 2011: Warm season afternoon thunderstorm characteristics under weak synoptic-scale forcing over Taiwan Island. *Weather and Forecasting*, **26,** 44-60.

National Academies of Sciences, E., and Medicine, 2016: *Attribution of extreme weather events in the context of climate change.* National Academies Press.

Pegion, K. V., and C. Selman, 2017: Extratropical Precursors of the El Niño–Southern Oscillation. *Climate Extremes: Patterns and Mechanisms*, 299-314.

Ren, F., G. Wu, W. Dong, X. Wang, Y. Wang, W. Ai, and W. Li, 2006: Changes in tropical cyclone precipitation over China. *Geophysical Research Letters*, **33**.

Shiu, C.-J., S. C. Liu, and J.-P. Chen, 2009: Diurnally Asymmetric Trends of Temperature, Humidity, and Precipitation in Taiwan. *Journal of Climate*, **22,** 5635-5649.

Tu, J.-Y., and C. Chou, 2013: Changes in precipitation frequency and intensity in the vicinity of Taiwan: typhoon versus non-typhoon events. *Environmental Research Letters*, **8,** 014023.

Wang, C.-C., G. T.-J. Chen, and R. E. Carbone, 2004: A climatology of warm-season cloud patterns over East Asia based on GMS infrared brightness temperature observations. *Monthly weather review*, **132,** 1606-1629.

Wang, S.-Y., and T.-C. Chen, 2008: Measuring East Asian Summer Monsoon Rainfall Contributions by Different Weather Systems over Taiwan. *Journal of Applied Meteorology and Climatology*, **47,** 2068-2080.

Wang, S.-Y., M. L'Heureux, and H.-H. Chia, 2012: ENSO prediction one year in advance using western North Pacific sea surface temperatures. *Geophys. Res. Lett.*, **39,** L05702.

Wang, S.-Y., M. L’Heureux, and J.-H. Yoon, 2013: Are greenhouse gases changing ENSO precursors in the Western North Pacific? Journal of Climate, 26, 6409-6322.

Wang, S. Y. S., Y.-H. Lin, and C.-H. Wu, 2016: Interdecadal change of the active-phase summer monsoon in East Asia (Meiyu) since 1979. *Atmospheric Science Letters*, **17,** 128-134.

Wu, C.-C., T.-H. Yen, Y.-H. Huang, C.-K. Yu, and S.-G. Chen, 2016: Statistical characteristic of heavy rainfall associated with typhoons near Taiwan based on high-density automatic rain gauge data. *Bulletin of the American Meteorological Society*, **97,** 1363-1375.

Xu, W., E. J. Zipser, and C. Liu, 2009: Rainfall characteristics and convective properties of mei-yu precipitation systems over South China, Taiwan, and the South China Sea. Part I: TRMM observations. *Monthly Weather Review*, **137,** 4261-4275.

Yeh, H.-C., and Y.-L. Chen, 1998: Characteristics of rainfall distributions over Taiwan during the Taiwan Area Mesoscale Experiment (TAMEX). *Journal of Applied Meteorology*, **37,** 1457-1469.

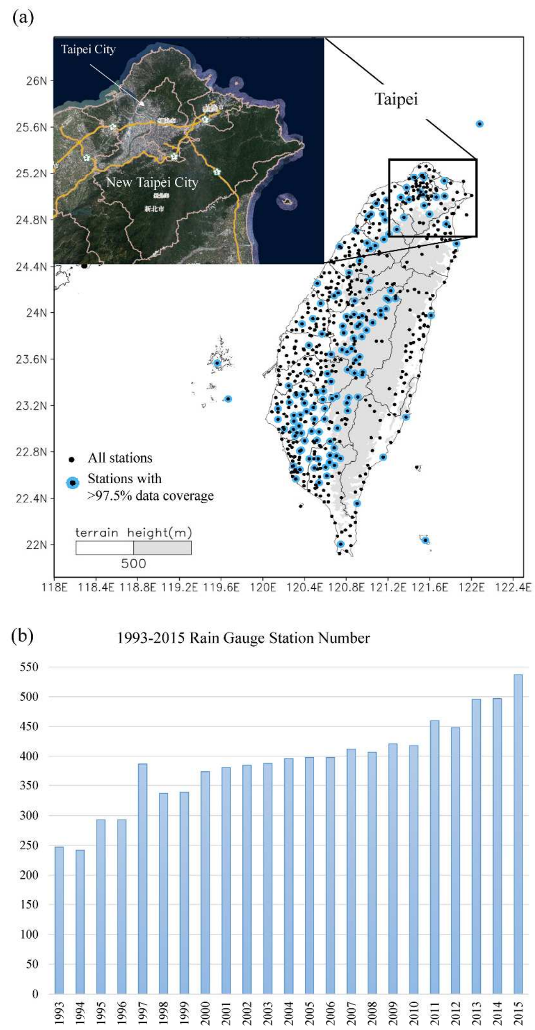

Figure 1

Figure 1. (a) Spatial distribution of the automated rain gauge stations in Taiwan from 1993 to 2015. Out of the 592 stations (black dots), only 135 stations (black dots superimposed by blue dots) provide data with at least 97.5% data coverage in the analysis period. The inset map depicts the location of Taipei, which consists of Taipei City and New Taipei City. (b) The growth of rain gauge station number from 1993 to 2015.

297x420mm (300 x 300 DPI)

(a)

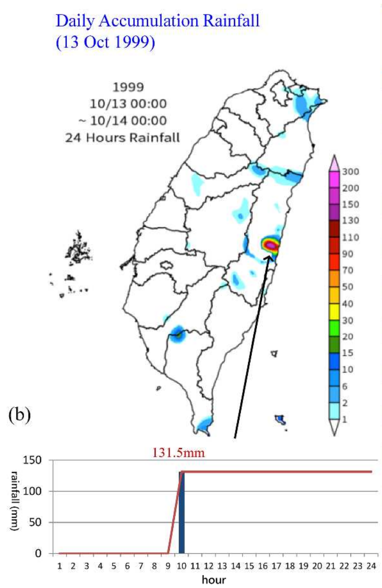

(c)

Date (yyyymmdd)	Hour	Station	Rainfall
19991013	1	C0T960	-9996
19991013	2	C0T960	-9996
19991013	3	C0T960	-9996
19991013	4	C0T960	-9996
19991013	5	C0T960	-9996
19991013	6	C0T960	-9996
19991013	7	C0T960	-9996
19991013	8	C0T960	-9996
19991013	9	C0T960	-9996
19991013	10	C0T960	**131.5**
19991013	11	C0T960	0
19991013	12	C0T960	0
19991013	13	C0T960	0
19991013	14	C0T960	0
19991013	15	C0T960	0
19991013	16	C0T960	0
19991013	17	C0T960	0
19991013	18	C0T960	0
19991013	19	C0T960	0
19991013	20	C0T960	0
19991013	21	C0T960	0
19991013	22	C0T960	0
19991013	23	C0T960	0
19991014	0	C0T960	0

Figure 2

Figure 2. An example of erroneous precipitation record due to radio miscommunication observed at Guangfu, Hualian on 13 Oct 1999. (a) The spatial distribution of daily precipitation (mm) on 13 Oct 1999. The location of Guanfu is indicated by the arrow. b) The hourly precipitation time series at Guangfu, Hualian. (c) The hourly precipitation record of 13 Oct 1999, where the record "-9996" indicates that the signal transmission was blocked and the accumulated rainfall will be recorded in the next hour.

297x420mm (300 x 300 DPI)

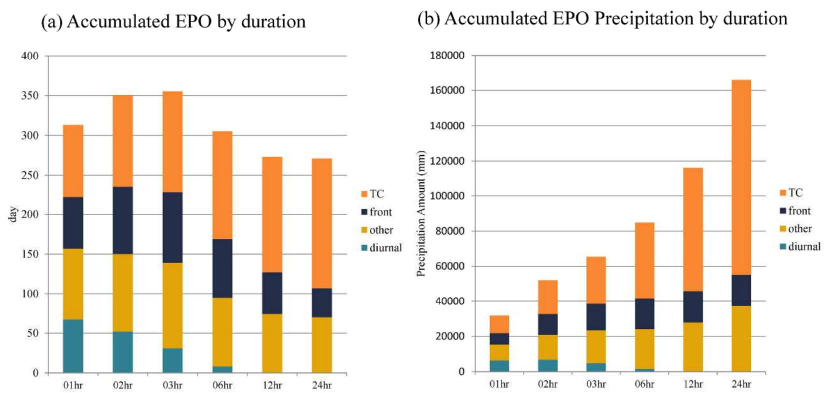

Figure 3

Figure 3. The frequency (day) of extreme precipitation occurrence (EPO) of 6 duration types, accumulated over 23 years from 1993 to 2015. Different colors indicate contribution from four major weather types. (b) As in (a) except showing the accumulated precipitation (mm) from EPOs.

297x420mm (300 x 300 DPI)

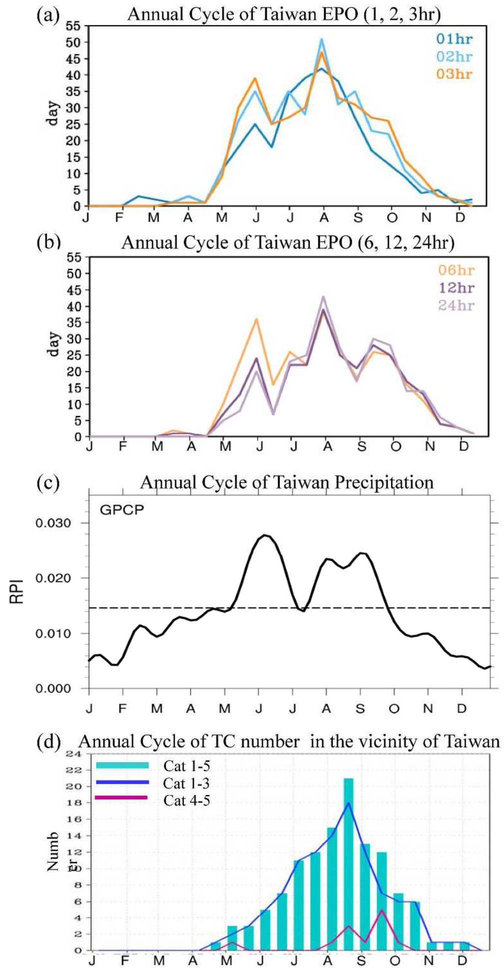

Figure 4. Half-month extreme precipitation occurrence (EPO) for durations from 1h, 2h, and 3h (a) and 6h, 12h, and 24h (b) accumulated over the 1993–2015 period. (c) The annual cycle of long-term pentad (5-day) precipitation using the GPCP data (Adler et al. 2003) averaged from the four grids surrounding Taiwan. (d) As in (a) except showing the number of tropical cyclones (from JMA's best track data) entering the vicinity of Taiwan, defined as the region within 300 km off the island's coastline. Blue bars denote all tropical cyclones, blue line category 1-3, and pink line category 4-5.

297x420mm (300 x 300 DPI)

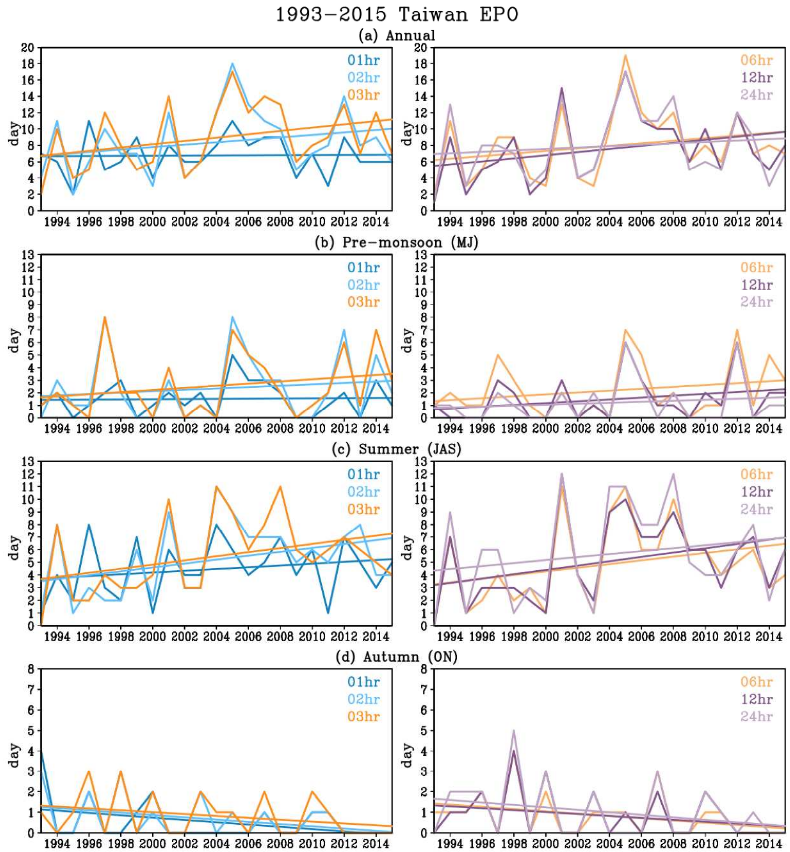

Figure 5. The interannual variations of the frequency (day) of Taiwan EPOs from 1993 to 2015 for 6 durations from 1h, 2h, and 3h (left) and 6h, 12h, and 24h (right). Frequency is accumulated over (a) the entire year, (b) pre-monsoon season (May-Jun), (c) summer (Jul-Aug-Sep), and (d) autumn (Oct-Nov). Linear trends (solid lines) of these EPOs are also superimposed.

297x420mm (300 x 300 DPI)

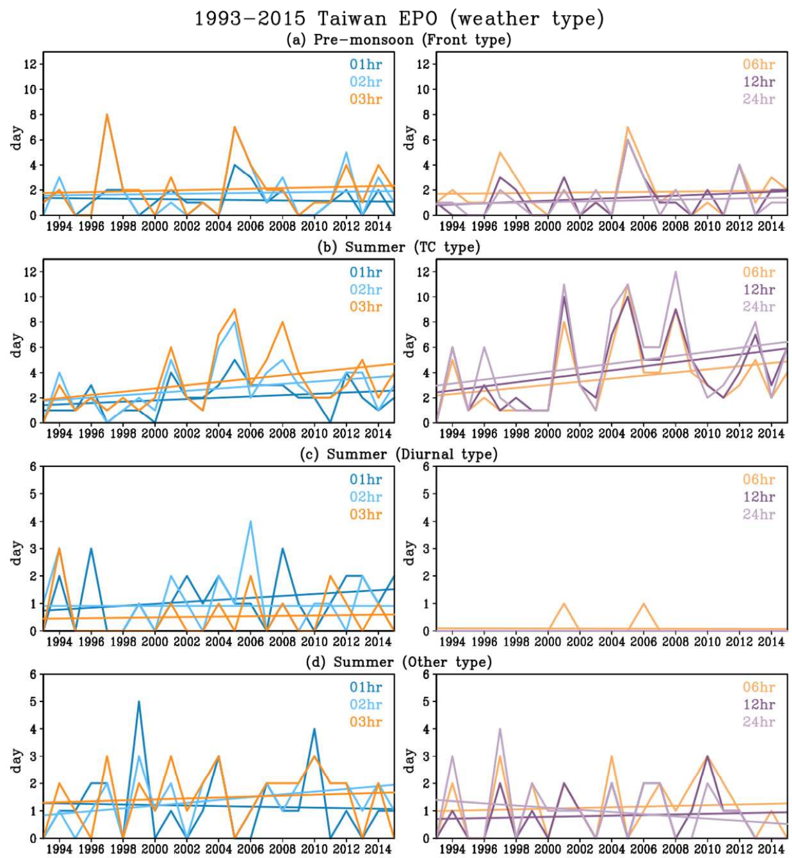

Figure 6. As in Figure 5 except for four major weather types in their primary seasons. (a) front type in pre-monsoon (May-Jun), (b) tropical cyclone type in summer (Jul-Aug-Sep), (c) diurnal type in summer (Jul-Aug-Sep), and (d) others type in summer (Jul-Aug-Sep).

297x420mm (300 x 300 DPI)

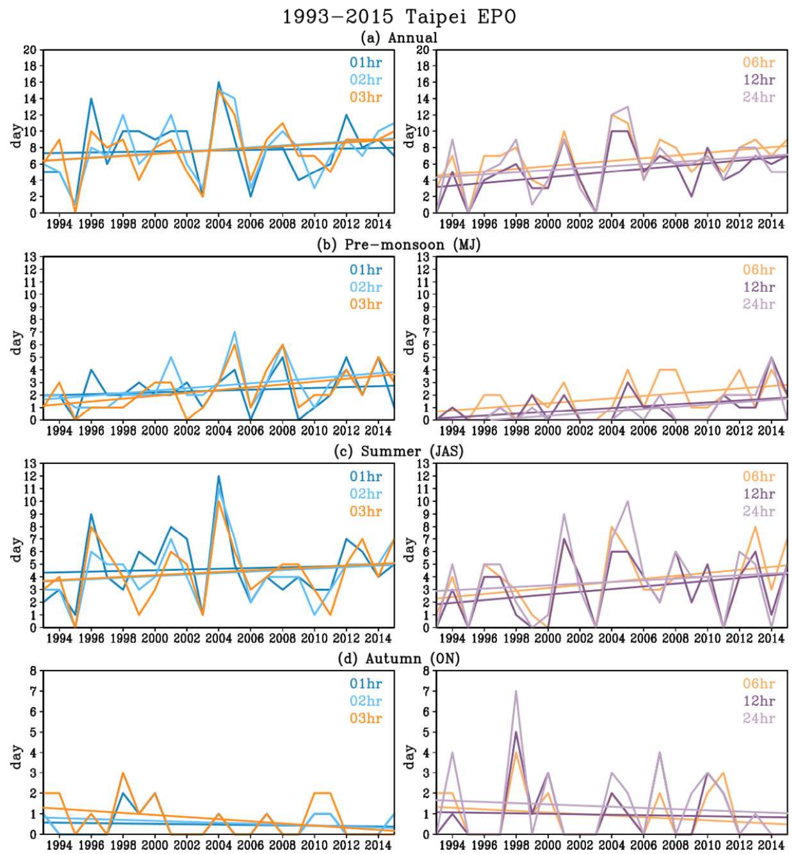

Figure 7. As in Figure 5 except for EPOs calculated over Taipei.

297x420mm (300 x 300 DPI)

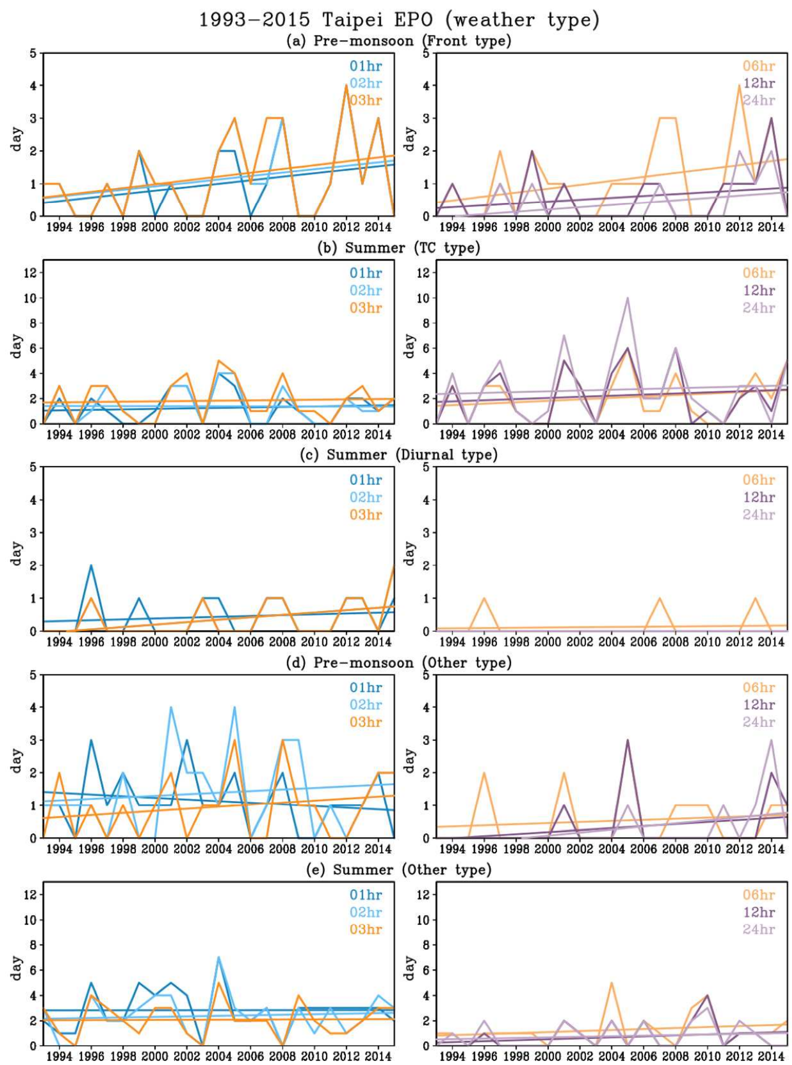

Figure 8. As in Figure 6 except for EPOs calculated over Taipei. One more panel (d) is included for the other type EPOs in pre-monsoon season (May-Jun).

297x420mm (300 x 300 DPI)

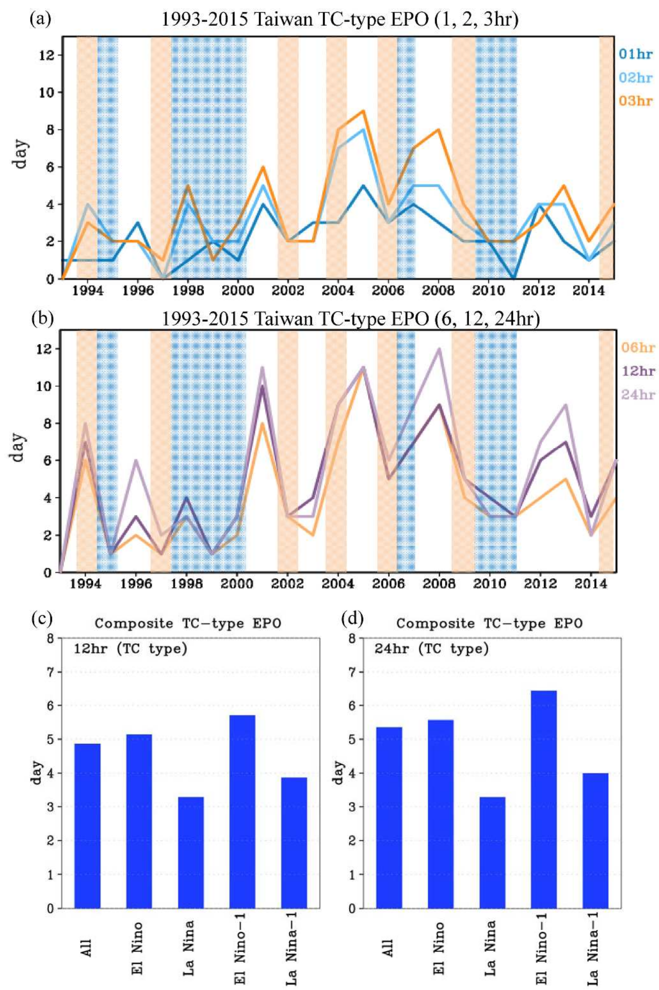

Figure 9. The interannual variations of the annual frequency (day) of TC-type EPOs from 1993 to 2015 for durations from 1h, 2h, and 3h (a) and 6h, 12h, and 24h (b). The composites of annual frequency (day) of TC-type EPOs for 23 (all) years, El Niño, La Niña, and their precursor years (El Nino-1 and La Nina-1) for the (c) 12h and (d)24h.

297x420mm (300 x 300 DPI)

Table 1

Type/Duration \ Season		Annual (Jan-Dec)	Pre-monsoon (May-Jun)	Summer (Jul-Sep)	Autumn (Oct-Nov)
All	1hr	0.008	0.007	0.070	**-0.056***
	2hr	0.149	0.055	**0.154***	**-0.055***
	3hr	**0.203**	0.085	**0.163***	**-0.045**
	6hr	0.157	0.075	**0.145**	**-0.055**
	12hr	**0.190**	**0.073**	**0.171***	-0.046
	24hr	0.087	0.040	0.118	**-0.060**
TC	1hr	0.045	-	0.052	-0.006
	2hr	0.063	-	**0.090**	-0.020
	3hr	**0.106**	-	**0.129***	-0.017
	6hr	**0.122**	-	**0.123**	-0.018
	12hr	**0.162***	-	**0.158***	-0.019
	24hr	**0.155**	-	**0.157**	-0.018
Front	1hr	-0.049	-0.014	-	-
	2hr	0.020	0.016	-	-
	3hr	0.037	0.026	-	-
	6hr	0.026	0.012	-	-
	12hr	0.048	0.050	-	-
	24hr	0.018	0.024	-	-
Diurnal	1hr	**0.043**	-	0.036	-
	2hr	0.005	-	0.000	-
	3hr	0.030	-	0.007	-
	6hr	0.010	-	-0.001	-
	12hr	-	-	-	-
	24hr	-	-	-	-
Other	1hr	-0.032	0.014	-0.010	**-0.040**
	2hr	**0.061**	**0.041***	**0.050**	-0.025
	3hr	0.031	**0.042***	0.017	-0.029
	6hr	0.000	**0.036***	0.013	**-0.039***
	12hr	-0.021	-	0.011	-0.022
	24hr	**-0.086***	-	-0.040	**-0.037**

Table 1. The 1993-2015 linear trends (day/year) of Taiwan EPOs of all as well as four major weather types for 6 durations. Trends are calculated either for annual frequencies or for seasonal frequencies. Levels of different statistical significances are indicated by special fonts or symbols. Trends in underlined fonts denote significance at 10% level, with * denote 5% level, and with ** denote 1% level.

297x420mm (300 x 300 DPI)

Table 2

Type/Duration \ Season		Annual (Jan-Dec)	Pre-monsoon (May-Jun)	Summer (Jul-Sep)	Autumn (Oct-Nov)
All	1hr	0.030	0.036	0.029	-0.009
	2hr	0.123	**0.099***	0.060	-0.023
	3hr	0.118	**0.113***	0.064	**-0.051***
	6hr	**0.166***	**0.098***	**0.120**	-0.039
	12hr	**0.174***	**0.077***	**0.109**	-0.012
	24hr	0.128	**0.092****	0.065	-0.029
TC	1hr	0.003	-	0.020	-0.017
	2hr	-0.012	-	-0.002	-0.017
	3hr	-0.007	-	0.013	**-0.027**
	6hr	0.037	-	0.056	**-0.027**
	12hr	0.034	-	0.044	-0.018
	24hr	0.020	-	0.032	-0.019
Front	1hr	0.032	**0.053**	-	-
	2hr	0.041	**0.052**	-	-
	3hr	**0.058**	**0.058**	-	-
	6hr	**0.070***	**0.060**	-	-
	12hr	**0.055***	0.029	-	-
	24hr	**0.047***	**0.036***	-	-
Diurnal	1hr	0.021	-	0.013	-
	2hr	**0.052***	-	**0.037***	-
	3hr	**0.052***	-	**0.037***	-
	6hr	0.018	-	0.004	-
	12hr	-	-	-	-
	24hr	-	-	-	-
Other	1hr	-0.026	-0.026	0.001	**0.019**
	2hr	0.042	0.024	0.021	0.005
	3hr	0.014	0.032	0.004	-0.014
	6hr	0.042	0.017	0.040	-0.002
	12hr	**0.074**	0.031	0.039	0.005
	24hr	0.058	**0.046***	0.023	-0.011

Table 2. Same as Table 1, except for EPOs calculated for Taipei.

297x420mm (300 x 300 DPI)